NBIT Final Report for AOARD Grant 104070

"PIEZOELECTRIC NANOGENERATORS FOR SELF-POWERED NANOSYSTEMS AND NANOSENSORS"

Date, May 15, 2013

Name of Principal Investigators (PI and Co-PIs): Zhong Lin Wang

- e-mail address : zhong.wang@mse.gatech.edu
- Institution : Georgia Institute of Technology
- Mailing Address : 500 10th street NW, Atlanta, GA 30332
- Phone : 404-894-8008
- Fax : 404-385-3852

Period of Performance: May/27/2010 – May/26/2013

Abstract:

The current rapid advancement of micro-/nanotechnology has gradually shift its focus from the development of discrete devices to the development of more complex integrated systems that are capable of performing multiple functions, such as sensing, actuating/responding, communicating, and controlling, by the integration of individual devices through state-of-the-art microfabrication technologies. Furthermore, it is highly desired for these multifunctional micro-/nanosystems (MNSs) to operate wirelessly and self-sufficiently without the use of a battery, especially in applications such as remote sensing and implanted electronics. This operation scheme will not only extend the life span and enhance the adaptability of these MNSs while greatly reducing the footprint and cost of the entire system, but it will also increase the adaptability of these MNSs to the environment in which they are deployed. As the dimensions of individual devices shrink, the power consumption decreases accordingly to a reasonably low level, so that energy scavenged directly from the ambient is sufficient to drive the devices. The concept of self-powered nanotechnology was first proposed and developed by the Wang research group at Georgia Institute of Technology, with the aim of building a system that operates by harvesting energy from the ambient vicinity of the system and converting it into usable electrical power for wireless, self-sufficient, and independent operations. A typical self-powered MNS should consist of a low-power microcontroller unit, high-performance data-processing/storage components, a wireless signal transceiver, ultrasensitive sensors based on micro-/nanoelectromechancial systems (MEMSs/NEMSs), and most importantly the embedded powering/energy-storage units.

In this project, intensive research effort has been invested in the development of self-powered MNSs, and various prototypes have been built up. Flexible piezotronic device based on RF-sputtered piezoelectric ZnO thin film is a great UV sensor. A nanogenerator based on the hydrothermal growth of a ZnO nanowire film on a spring shows a stable output and both the output voltage and current, displaying a linear relationship with the weight loaded on the spring. Thus, the nanogenerator can be utilized as an active mechanical sensor for measuring the weight applied onto the spring. A flexible thermoelectric nanogenerator (TENG) can be used as a wearable energy harvester by using human body temperature as the energy source. At the same time, the TENG can work as a self-powered temperature sensor

Report Documentation Page

Form Approved
OMB No. 0704-0188

1. REPORT DATE **30 MAY 2013**	2. REPORT TYPE **Final**	3. DATES COVERED **01-05-2010 to 04-05-2013**
4. TITLE AND SUBTITLE **High output nanogenerators for self-powered nanosensors (NBIT Phase II)**		5a. CONTRACT NUMBER **FA23861014070**
		5b. GRANT NUMBER
		5c. PROGRAM ELEMENT NUMBER
6. AUTHOR(S) **Zhong Lin Wang**		5d. PROJECT NUMBER
		5e. TASK NUMBER
		5f. WORK UNIT NUMBER
7. PERFORMING ORGANIZATION NAME(S) AND ADDRESS(ES) **Georgia Institute of Technology,771 Ferst Drive,Atlanta,GA,30332-0245**		8. PERFORMING ORGANIZATION REPORT NUMBER **N/A**
9. SPONSORING/MONITORING AGENCY NAME(S) AND ADDRESS(ES) **AOARD, UNIT 45002, APO, AP, 96338-5002**		10. SPONSOR/MONITOR'S ACRONYM(S) **AOARD**
		11. SPONSOR/MONITOR'S REPORT NUMBER(S) **AOARD-104070**
12. DISTRIBUTION/AVAILABILITY STATEMENT **Approved for public release; distribution unlimited**		
13. SUPPLEMENTARY NOTES		

14. ABSTRACT

14. ABSTRACT In this project, intensive research effort has been invested in the development of self-powered MNSs, and various prototypes have been built up. Flexible piezotronic device based on RF-sputtered piezoelectric ZnO thin film is a great UV sensor. A nanogenerator based on the hydrothermal growth of a ZnO nanowire film on a spring shows a stable output and both the output voltage and current, displaying a linear relationship with the weight loaded on the spring. Thus, the nanogenerator can be utilized as an active mechanical sensor for measuring the weight applied onto the spring. A flexible thermoelectric nanogenerator (TENG) can be used as a wearable energy harvester by using human body temperature as the energy source. At the same time, the TENG can work as a self-powered temperature sensor with a response time of 17 s and a reset time of 9 s. The detection sensitivity of the sensor can reach 0.15 K in ambient atmosphere. The single output peak from a pyroelectric nanogenerator (PENG) based on a lead zirconate titanate (PZT) film can be used to directly drive a LCD. Further, a homemade Li-ion battery can be charged by the PENG under different working frequencies from 0.005 to 0.02 Hz, which can be used to drive a green LED. An integrated module in the form of a combination of a nanoparticle-WO3 film electrochromic device and a nanogenerator demonstrates the potential of monochrome self-powered displays. This self-powered electrochromic device showed desirable electrochromic response times and high coloration efficiency values. A transparent flexible nanogenerators made by growing ZnO nanowires on flexible polydimethylsiloxane (PDMS) substrate is a self-powered sensor for monitoring vehicle speed and detecting vehicle weight. Using two kinds of piezoelectric material, ZnO and poly-(vinylidene fluoride) (PVDF), we fabricate a composite structure for a nanogenerator (NG) or active-sensor for mechanical energy harvesting and vortex-based gas/liquid flow measurements. The studies carried out in this project have inspired rapid progress in the field of self-powered micro-/nanotechnology worldwide in applications ranging from corrosion monitoring to distributed sensing and environmental monitoring.

15. SUBJECT TERMS

16. SECURITY CLASSIFICATION OF:			17. LIMITATION OF ABSTRACT	18. NUMBER OF PAGES	19a. NAME OF RESPONSIBLE PERSON
a. REPORT **unclassified**	b. ABSTRACT **unclassified**	c. THIS PAGE **unclassified**	**Same as Report (SAR)**	**13**	

with a response time of 17 s and a reset time of 9 s. The detection sensitivity of the sensor can reach 0.15 K in ambient atmosphere. The single output peak from a pyroelectric nanogenerator (PENG) based on a lead zirconate titanate (PZT) film can be used to directly drive a LCD. Further, a homemade Li-ion battery can be charged by the PENG under different working frequencies from 0.005 to 0.02 Hz, which can be used to drive a green LED. An integrated module in the form of a combination of a nanoparticle-WO_3 film electrochromic device and a nanogenerator demonstrates the potential of monochrome self-powered displays. This self-powered electrochromic device showed desirable electrochromic response times and high coloration efficiency values. A transparent flexible nanogenerators made by growing ZnO nanowires on flexible polydimethylsiloxane (PDMS) substrate is a self-powered sensor for monitoring vehicle speed and detecting vehicle weight. Using two kinds of piezoelectric material, ZnO and poly-(vinylidene fluoride) (PVDF), we fabricate a composite structure for a nanogenerator (NG) or active-sensor for mechanical energy harvesting and vortex-based gas/liquid flow measurements.

The studies carried out in this project have inspired rapid progress in the field of self-powered micro-/nanotechnology worldwide in applications ranging from corrosion monitoring to distributed sensing and environmental monitoring.

Introduction:

With the growing threat of pollution, global warming, and energy crises caused by our strong dependence on the dwindling supply of nonrenewable fossil fuels, the search for clean and renewable alternative energy resources is one of the most urgent challenges to the sustainable development of human civilization. In addition to the energy resources which drive human society today, such as petroleum, coal, hydraulic power, natural gas, wind power, and nuclear plants, a focus of active research and development is the exploration of alternative sustainable energy resources, such as solar energy, geothermal power, biomass/biofuel, and hydrogen energy. Although there is potential for the use of these alternative sources for the large-scale supply of power, the energy that can be harvested from these sources is still mainly used for small-scale powering applications.

A dramatic technological trend today is the rapid growth of personal and mobile electronics for applications in communication, health care, and environmental monitoring. Individually, the power consumption of these electronics is low; however, the number of such devices deployed can be huge. Currently, the powering of electronic devices still relies on rechargeable batteries. The amount of batteries required increases in proportion with the increase in the number and density of mobile electronic devices used and may result in challenges for recycling and replacement of the batteries as well as concerns about potential environmental pollution. To effectively extend the lifetime of batteries and even completely replace batteries in some cases, a worldwide effort has begun towards the development of technologies for harvesting energy from our living environment, such as solar energy, thermoelectricity, mechanical vibration, and biofuels. The first target is to power sensors and micro-/nanosystems (MNSs).

Intensive efforts during the last two decades towards the design and development of micro-/nanotechnology for various applications have led to systems with unprecedented performance, as enabled by improved capabilities in materials synthesis and increasingly sophisticated micro-/nanofabrication technologies. Although micro-/nanodevices require much lower power consumption than their conventional counterparts, the powering of these systems can still be challenging. Almost all reported MNSs are powered by a traditional power cord or battery, which is in general much larger than the device being powered and hence dictates the size of the entire system. This conventional power-supply scenario also leads to issues of replacement/maintenance, cost, and environmental concerns, and severely hinders the further development and practical deployment of micro-/nanotechnology. A nanosystem should therefore consist of not only functional nanodevices but also nanoscale power sources. The dilemma is, however, that the miniature size of these power sources can largely limit their lifetime and efficiency. The design and development of appropriate energy-harvesting strategies for miniaturized powering packages is thus critical to the fulfillment of the potential and promises of micro-/nanotechnology.

Research on micro-/nanotechnology in the near future should therefore be aimed at integrating micro-/nanodevices into multifunctional systems capable of wireless, self-sufficient, and intelligent operations, such as sensing, actuating/responding, communicating, and controlling. It is highly desirable for MNSs to be **self-powered** without a battery, particularly for applications such as remote sensing and implanted biomedical systems, as the life span of the devices would thus be extended, the footprint and cost of entire system decreased, and the adaptability of these MNSs to the environment increased. The development of enabling technology for harvesting energy from the environment and converting it into usable electric power to support the self-sufficient operation of MNSs is the most promising strategy to overcome the current challenges and hurdles presented by conventional powering methods. In contrast to energy stored in storage elements, such as batteries and capacitors, the environment can be viewed as an almost infinite reservoir of energy available for potential applications. The goal of energy-harvesting technologies for self-powered MNSs is thus to develop power sources which operate over a broad range of conditions for extended time periods with high reliability.

The current rapid advancement of micro-/nanotechnology will gradually shift its focus from the development of discrete devices to the development of more complex integrated systems that are capable of performing multiple functions, such as sensing, actuating/responding, communicating, and controlling, by the integration of individual devices through state-of-the-art microfabrication technologies. Furthermore, it is highly desired for these multifunctional MNSs to operate wirelessly and self-sufficiently without the use of a battery, especially in applications such as remote sensing and implanted electronics. This operation scheme will not only extend the life span and enhance the adaptability of these MNSs while greatly reducing the footprint and cost of the entire system, but it will also increase the adaptability of these MNSs to the environment in which they are deployed. As the dimensions of individual devices shrink, the power consumption decreases accordingly to a reasonably low level, so that energy scavenged directly from the ambient is sufficient to drive the devices. The concept of **self-powered nanotechnology** was first proposed and developed by the Wang research group with the aim of building a system that operates by harvesting energy from the ambient vicinity of the system and converting it into usable electrical power for wireless, self-sufficient, and independent operations. A typical self-powered MNS should consist of a low-power microcontroller unit, high-performance data-processing/storage components, a wireless signal transceiver, ultrasensitive sensors based on micro-/nanoelectromechancial systems (MEMSs/NEMSs), and most importantly the embedded powering/energy-storage units.

This project focuses on both the scientific understanding and technology development of energy harvesting specifically for powering future functional MNSs. Some representative achievement listed below in this report include: 1. Piezotronic effect in flexible thin-film based devices; 2. Elastic-spring-substrated nanogenerator as an active sensor for self-powered balance; 3. Nanowire-composite based flexible thermoelectric nanogenerators and self-powered temperature Sensors; 4. Pyroelectric nanogenerators for driving wireless temperature sensors; 5. A self-powered electrochromic device driven by a nanogenerator; 6. Transparent flexible nanogenerator as self-powered sensor for transportation monitoring; 7. Nanogenerators as an active sensor for vortex capture and ambient wind-velocity detection.

Results and Discussion:

1. **Piezotronic Effect in Flexible Thin-film Based Devices**

Flexible piezotronic device based on RF-sputtered piezoelectric semiconductor thin films has been investigated for the first time. The dominating role of piezotronic effect over geometrical and piezoresistive effect in the as-fabricated devices has been confirmed and the modulation effect of piezopotential on charge carrier transport under different strains is subsequently studied. Moreover, we also demonstrate that UV sensing capability of as-fabricated thin film based piezotronic device can be tuned by piezopotential, showing significantly enhanced sensitivity and improved reset time under tensile strain. It is prospected that piezoelectric semiconductor thin films can be an excellent alternative to their 1D counterpart for realizing piezotronic applications due to the technological compatibility with state-of-art microfabrication technology. Results demonstrated here broaden the scope of piezotronics and extend its potential applications in fields of sensors, flexible electronics, flexible ptoelectronics, smart MEMS/NEMS and human-machine interfacing.

The structure of the polycrystalline ZnO thin film grown by RF sputtering onto PET substrates is characterized in Figure 1. While the ZnO piezotronic thin film based UV sensor was demonstrated in Figure 2 and the feasibility of modulating its UV sensing capability by externally applied strain has been investigated. A 365-nm UV lamp was used in the experiment. For each test, UV light was turned on for 1s and then switched off, while the temporal response of current from the device was monitored under bias of 5 V. In Figure 2 a, the black curve was recorded when no strain was applied to the device, showing a sensitivity (defined as the percentage increase of current values) of 25% and a reset time of ~ 880 s. When 0.24% tensile strain was applied, an apparent enhancement of sensitivity was observed, from 25% to 89.25% with a shorter reset time of 582 s, as shown by the blue curve. When the applied tensile strain was increased to 0.48% (the red curve), the UV sensitivity further increased to as high as 112.5% with an even shorter reset time of 337 s. The cases for device under compressive strains are also obtained and plotted in Figure 2 b for comparison. When -0.24% compressive strain was applied, the device sensitivity decreased from 25% to 13.21% (green line). As the applied compressive strain was increased to -0.48%, as shown by the orange curve, the sensitivity further decreased to 12.9%. The corresponding reset time increased to over half an hour for both cases. The tuning effect of strain on device's UV sensitivity is summarized in Figure 2 c and a significant enhancement of sensitivity by applying tensile strain can be observed.

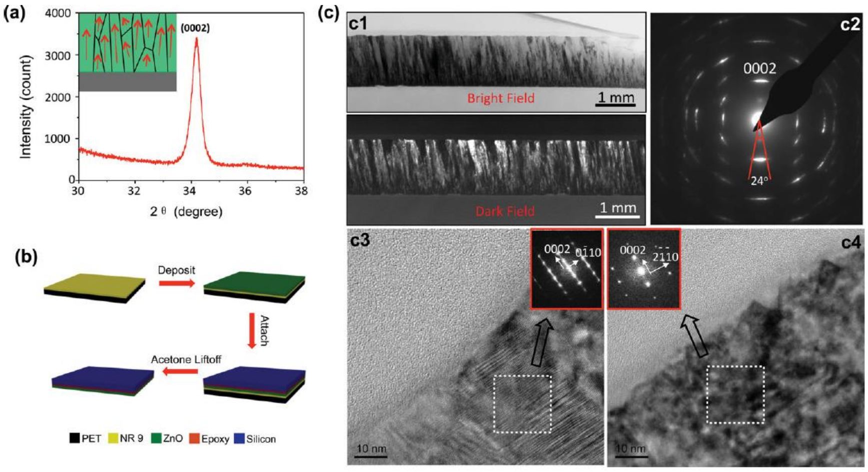

Figure 1 Structure characterization of the polycrystalline ZnO thin fi lm grown by RF sputtering onto PET substrates.

In addition to the direct contribution from photon-generated excess carriers, ZnO has another important mechanism that contributes to its UV sensing capability. In dark environment, oxygen can be adsorbed onto ZnO surface through the reaction [$O_2 + e^- \longrightarrow O_2^-$]. Since free electrons are consumed by this adsorption, a depletion layer is consequently created that decreases the conductivity near the fi lm surface. Upon UV illumination, excess electron-hole pairs will be generated and the generated holes can discharge the adsorbed oxygen ions, leading to the increase of surface conductivity. Meanwhile, with the accumulation of excess electrons, oxygen will be re-adsorbed and finally a new equilibrium is reached. When the illumination is turned off, electrons and holes will start to recombine with each other. This recombination process can, however, be very slow due to the hole trapping effects at the surface, mitigating the re-adsorption of oxygen, which explains the long reset time normally observed in ZnO based UV sensors. The above mechanism applies to the situation where bare ZnO is exposed to UV light. For our device, in addition to the above processes, the Schottky barriers formed between Au electrodes and ZnO also come into play by introducing a strong local electric field across the interface. Immediately after electron-hole pairs are generated upon UV illumination, they will be effectively separated by this local electric field, which reduces the recombination rate and increases the carrier lifetime and density. As a result, oxygen can be discharged and desorbed at a faster rate. Meanwhile, the SBH is decreased due to illumination so that more charge carriers can transport through the barrier region. These factors all lead to the enhanced sensitivity observed for Schottky-contact based ZnO UV sensors. When UV illumination is turned off, this local electric fi eld can quickly restore the carrier distribution to its original status, overcoming the trapping effect, and hence lead to a shorter reset time.

When strain is introduced into the system, the induced piezoelectric polarization charges can also effectively modulate the above processes, as shown by the schematics and band diagrams in Figure 2 c. When tensile strain is applied (region in light yellow), negative polarization charges are induced at the top surface, promoting the oxygen adsorption/re-adsorption process, which contributes to the observed increased UV sensitivity and decreased reset time. Moreover, the induced negative piezopotential will raise the SBHs on both electrodes, resulting in further improvement to the UV sensing performance. On the other hand, when compressive strain is applied (region in light blue), the induced positive polarization charges at the surface will partially deplete the free electrons in the surface region, mitigating the oxygen adsorption/re-adsorption process, and hence decrease the UV sensitivity and increase the reset time. The positive ionic polarization charges at the semiconductor-metal interface can also lower the SBHs and furtherdegrade the UV sensing performance.

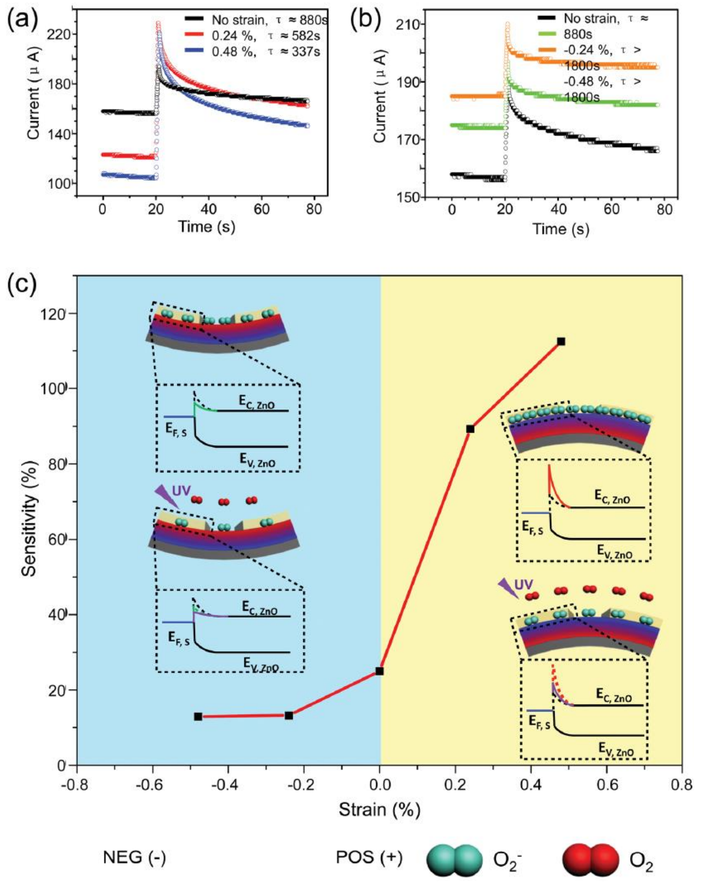

Figure 2 ZnO piezotronic thin film based UV sensor with tunable sensing capability. The color gradient at the bottom represents the strain induced piezopotential. (a) Tensile strains are applied to the device which increases the UV sensitivity and decreases the reset time. (b) Compressive strains are applied to the device which decreases the UV sensitivity and increases the reset time. (c) Sensitivity of the UV sensor under different strain values. The insets explain the underlying mechanism of the strain tuning effect.

2. Elastic-spring-substrated nanogenerator as an active sensor for self-powered balance

We give a novel design of a piezoelectric nanogenerator that is monolithically integrated onto an elastic spring by growing ZnO nanowire arrays on the surface of the spring. Under a cyclic compressive force applied to the spring, the nanogenerator produced a stable AC output voltage and current, which are linearly responding to the applied weight on the spring. By conjunction of the experimental data with finite element simulation, we show that the output open-circuit voltage of the nanogenerator can serve as an active sensor for a self-powered weight measurement system. By active sensor we mean that the sensor automatically gives an electric output signal without applying an external power source, which can be used to directly quantify the mechanical triggering applied onto the nanogenerator.

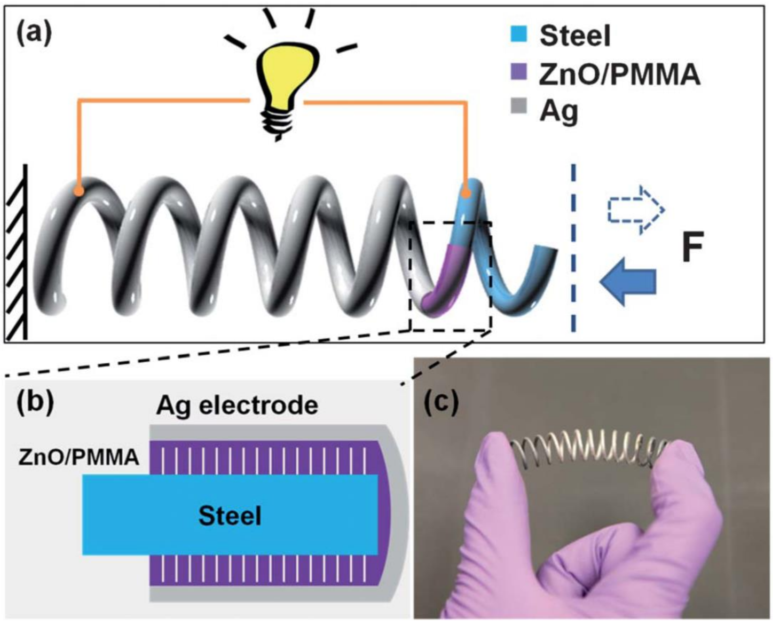

Figure 3 (a) Schematic structure of the spring-substrated nanogenerator, in which a textured piezoelectric ZnO nanowire film is grown on the surface of the elastic wire. (b) A cross-sectional schematic illustration of the nanogenerator showing its detailed structure, which is composed of a steel spring (substrate and inner electrode), ZnO nanowire film, PMMA insulating layer, as well as the outer Ag electrode. (c) A photograph of the spring-substrated nanogenerator.

The structure and general working principle of the spring-substrated nanogenerator (SNG) are schematically shown in Fig. 3a–c. Compressive springs with variable sizes were selected as the skeletons of the SNG devices. The helix-shaped spring surface was composed of high carbon steel, which was taken as the substrate for the growth of ZnO NWs and was also employed as the inner electrode due to the conductive nature of the steel. The ZnO NWs were grown by the wet chemical approach on the treated spring surface. The NWs were uniformly grown on the spring and densely packed as a textured lm with the c-axes of the NWs pointing outward. The as-synthesized NW film was coated with polymethyl methacrylate (PMMA) as a buffer layer and deposited with silver as the outer electrode. Both the inner and outer electrodes were connected to the external measurement circuit by copper electric leads, and the whole device was encapsulated with polydimethylsiloxane (PDMS) to protect the electrode.

In the measurement for the output performance of the SNG, one end of the spring was fixed onto a three-dimensional stage; meanwhile a mechanical linear motor was employed to apply a periodic longitudinal compressive force to the SNG. As the compressive force is applied onto the spring, the strain-induced piezoelectric potential (piezopotential) in ZnO will be created and drive the electrons flowing in the external load until the accumulated electrons reach equilibrium with the piezopotential; once the applied force is released, the piezopotential diminishes and the accumulated electrons will flow back in the opposite direction, which leads to an AC current. With an applied compressive force of 15.2 N (the corresponding displacement of the spring is 10 mm), for a spring with spring constant of 1.52 Nmm^{-1}, the output open-circuit voltage and short-circuit current of the SNG was _0.23 V and

5 nA, respectively. The stability of its output performance was also tested through continuously loading and unloading the periodic force for three days at a frequency of 0.32 Hz. It can be found that the output of the SNG only showed a decay of 3–4% after three days of continuous working (corresponding to ~80000 cycles), owing to the high flexibility of the ZnO NWsand thus the high robustness of the SNG device. The stability of the SNG's output ensures its application as an active mechanical sensor.

In summary, both the output voltage and current displayed a linear relationship with the equivalent applied weight to the spring, and the weight measurement was validated by comparison with other factors like loading rate of the force, spring size, and impact frequency. Our study shows that the output voltage of the nanogenerator could be utilized as an active sensor signal for a self-powered weight measurement system, which can be further employed in transportation monitoring.

3. Nanowire-Composite based Flexible Thermoelectric Nanogenerators and Self-Powered Temperature Sensors

We have developed a flexible thermoelectric nanogenerator (TENG) that is based on a Te-nanowire/poly (3-hexylthiophene) (P3HT) polymer composite as the thermoelectric material with a positive Seebeck coefficient of 285 μV/K. A linear relationship between the output voltage of TENG and the temperature difference across the device was observed. Under a temperature difference of 55 K, two TENGs can provide an output voltage of 38 mV in serial connection, or a current density exceeding 32 nA/mm^2 in parallel connection. We demonstrated that the flexible TENG can be used as a wearable energy harvester by using human body temperature as the energy source. In addition, the TENG can also be used as a self-powered temperature sensor with a response time of 17 s and a reset time of 9 s. The detection sensitivity of the sensor can reach 0.15 K in ambient atmosphere.

The fabricated TENGs are very flexible and can be attached on any substrate (such as Kapton film), as shown in Fig. 4(a). Measurements made using the TENG are shown schematically in Fig. 4(b). A thin poly(dimethylsiloxane) (PDMS) layer was used to package the TENG to avoid any effects of the atmosphere. Two heaters with a distance of 6 mm were fixed on the two electrodes. The right heater was kept at room temperature and connected with the positive electrode of the measurement system. Figure 4(c) shows that the output voltage linearly increased with increasing temperature difference across the TENG. The calculated Seebeck coefficient is about 285 μV/K.

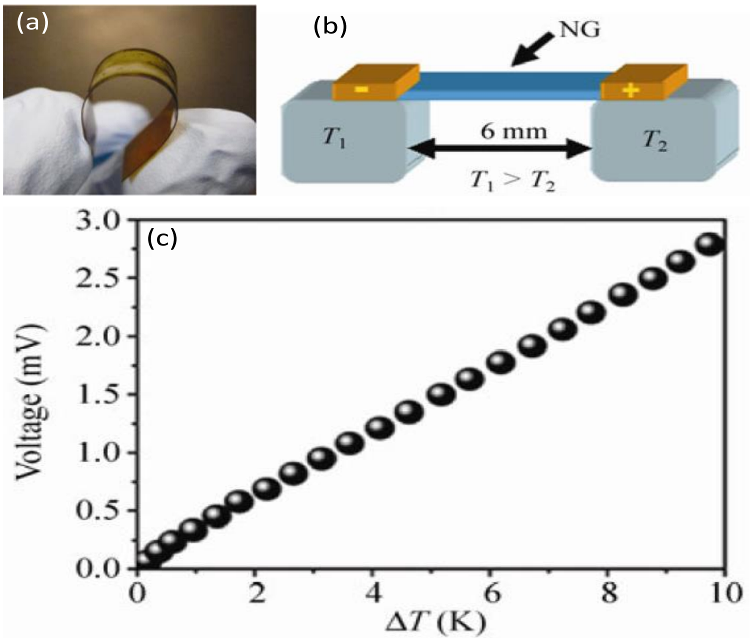

Figure 4 (a) Photograph of a Te-nanowire/P3HT-polymer composite device on a flexible Kapton substrate. (b) Schematic diagram of the measurements. (c) The output voltage of the TENG as a fu nction of change in temperature difference across the device

4. Pyroelectric Nanogenerators for Driving Wireless Temperature Sensors

We have been developing nanogenerators for build self-powered systems that can operate independently and wirelessly without the use of a battery or other energy storage/supply. One of the great applications for the self-powered system is to use nanogenerators to drive personal electronics, such as LCDs and LEDs. Currently, piezoelectric NGs have been used to drive some electrical devices by harvesting mechanical energy from the environment. Although different designs of pyroelectric nanogenerators (PENGs) have been reported, the output voltage and current of these devices are still very low (voltage below 0.1 V, and current below 1 nA), which are not enough for driving any commercial electronics. To solve this problem, the performance optimization of the PENGs is desperately needed. Here, we demonstrated a lead zirconate titanate (PZT) film PENG, where the output open-circuit voltage and short-circuit current density can be up to 22 V and 171 nA/cm2, respectively. Under a change in temperature of 45 K, a single output pulse of PENG can continuously drive a LCD for longer than 60 s. A Li-ion battery can be charged by such PENGs under different frequencies.

Our design of the PENG is based on the change in spontaneous polarization of a PZT thin film due to the time-dependent temperature fluctuation to drive electrons to flow in external circuit. The detailed fabrication method of the PENG is given in the Experimental Section. Figure 5a shows an optical image of the fabricated PENG, indicating that the device has a length of 21 mm and a width of 12 mm. Figure 5b shows a cross-sectional scanning electron microscopy (SEM) image of the device, revealing the thickness of the device to be 175 μm. The large size PZT microfilm was chosen for easy manipulation. The same principle and methodology can be applied to the PZT nanofilm. The enlarged SEM image of the cross section indicates that the film consists of a large number of crystal grains, as shown in Figure

5c. The output voltage and current of the PENG have been measured by varying the temperature in the vicinity of the NG from 295 to 299 K, as shown in Figure 5d. The corresponding differential curve of the change in temperature with time shows that the peak value of the temperature changing rate is about 0.2 K/s. Under the forward connection, a sharp negative voltage/current pulse (~2.8 V; 42 nA) was observed when the temperature was quickly increased from 295 to 299 K (Figure 1e), and a corresponding positive pulse was received when the temperature was recovered back to 295 K (Figure 5e). After reversely connecting the PENG to the measurement system, the opposite signals were observed, suggesting that the measured signals were generated by the PENG. Usually, the pyroelectric current I can be described as I = pA(dT/dt), where p is the pyroelectric coefficient, A is the electrode area, and dT/dt is the rate of change in temperature. According to this equation, the current will linearly increase with increasing the rate of change in temperature, which is consistent with the experimental results. From the above results, the obtained pyroelectric coefficient of PZT film is about −80 nC/cm^{2}K, which is much larger than that of ZnO.

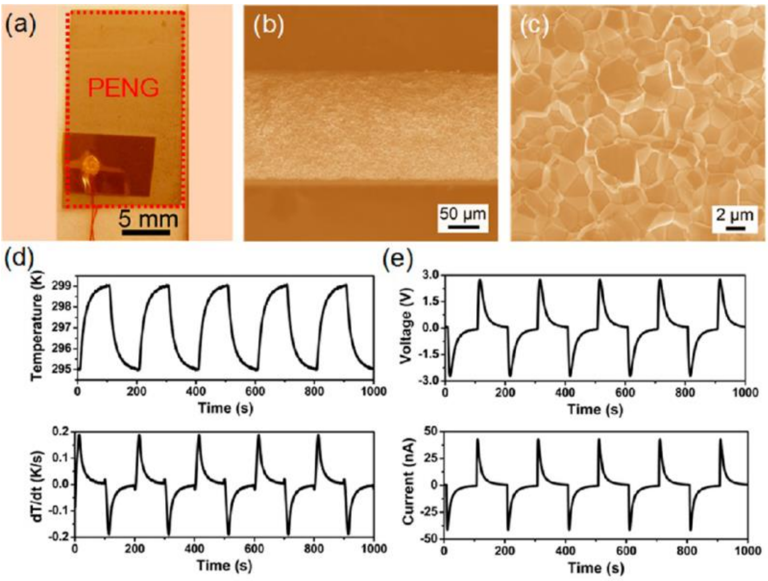

Figure 5 (a) Photograph of a fabricated PENG. (b) Cross-sectional SEM image of the PENG. (c) Enlarged Cross-sectional SEM image of the PENG. (d) The cyclic change in temperature of the PENG and the corresponding differential curve. (e) Measured output voltage and current of the PENG under the change in temperature in d.

To illustrate the potential applications of the PENGs, we demonstrated that they may be used as the power sources for wireless sensors. Figure 6a shows a wireless temperature sensor system, which includes the temperature sensor, the signal processing unit, and the flexible antenna. It can be driven by a rechargeable Li-ion battery with a voltage of 2.8 V, as shown in the inset of Figure 6a. Figure 6b shows the received signal from the wireless temperature sensor, indicating that the temperature at that time was about 296.2 K. Figure 6c shows the change in temperature in about a half an hour recorded by the wireless temperature sensor with each data for 1 min. The working distance of the wireless sensor can be larger than 50 m. Currently, the Li-ion battery still cannot be charged to 2.8 V by the fabricated PENG since the obtained current is not large enough to completely overwhelm the universally existing self-discharge of the battery. To increase the output current of the PENG, one possible method is to increase the area of the device according to equation of I =

pA(dT/dt). Figure 6d shows the output current of a new device is up to 0.8 μA, which is two times larger than that of the device in Figure 2b, where the corresponding area is two times larger than that of PENG in Figure 2b. By using the output voltage and current equations of the PENG, we can find that the increase of both the pyroelectric coefficient and the change in temperature can enhance both the output voltage and the current. Moreover, the output voltage can be improved by increasing the thickness of the PZT film.

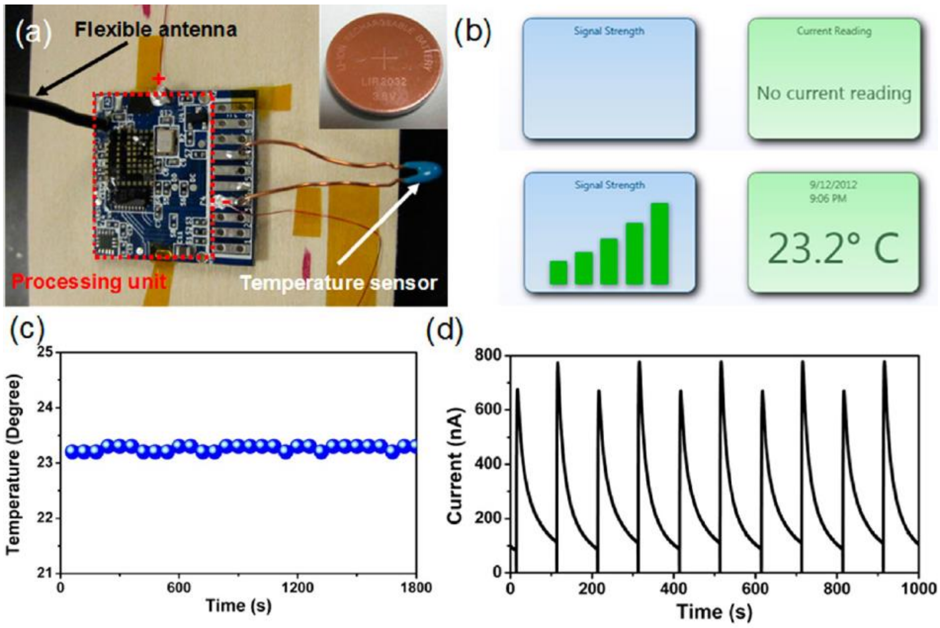

Figure 6 (a) Photograph of a wireless temperature sensor. The inset shows the photograph of a rechargeable Li-ion battery. (b) The obtained temperature signals when the wireless temperature sensor was turned off and on. (c) The obtained temperature data in half an hour, where the temperature value was recorded in every 1 min. (d) Output current of the new PENG when the surface area of the device was increased to 2 times as compared with that in Figure 2b.

5. A self-powered electrochromic device driven by a nanogenerator

Electrochromic (EC) materials are capable of reversibly changing optical properties upon charge injection and extraction, which are driven by an externally applied voltage. They are currently attracting much interest because of low power consumption and high coloration efficiency that make them suitable for a variety of applications such as smart windows, electronic billboards, as well as displays of portable and flexible devices including smart cards, price labels and electronic papers. For example, tungsten trioxide (WO3), when injected with protons or other small monovalent cations such as Li^+, becomes dark blue with little power involved. Even lower power consumption is expected if WO3 nanoparticles are used for the electrochromic purpose. Therefore, it is entirely possible to drive the electrochromic device by nanogenerators that scavenge energy from the environment such as airflow, vibration, sonic waves, human activity and so on. In this paper, we developed two kinds of selfpowered systems by integrating a WO3-based electrochromic device with a nanogenerator for potential applications in monochrome selfpowered displays in portable electronic devices as well as in electronic billboards.

Fig. 7 a and b show schematic diagrams of self-powered EC systems. The power source unit has an NG and a full-wave bridge for rectification. The NG converts mechanical energy into electricity, while the full-wave bridge transforms alternating current from the NG to unidirectional current. In this work, two types of self-powered EC systems are designed. In the first approach, the electricity generated by the NG is rectified and stored in a capacitor and then released to drive the EC device (Fig. 7a). The charging process and discharge process are controlled by a regular switch (blue dashed rectangle in Fig. 7a). A reversible switch is for determining how the capacitor and the EC device are connected. In the second design, the NG was connected to the EC device through a full-wave rectifier without an energy storage unit as an in situ power supply (Fig. 2b). There is also a reversible switch for reversing the connection polarity between the NG and the EC unit.

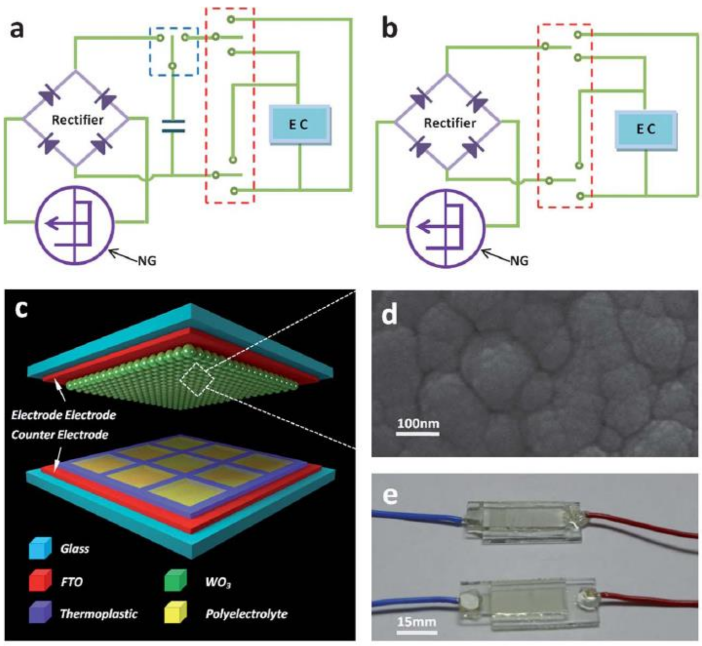

Figure 7 Schematic diagram of the self-powered electrochromic device (EC) system and the structure of theWO3-based EC device. (a) NG-charged power source; (b) real-time power supply; (c) the structure of the WO3-based EC device; (d) SEM image of the WO3 film; (e) a picture of the EC device.

The EC unit has a multi-layered structure, which is sketched in Fig. 7c. The outer layers are commercially purchased glass substrates covered with FTO thin films on one side as electrodes, which have a sheet resistance and transmittance of 35–45 Ω per sq. and 80%, respectively. Until otherwise noted, all transmittance data in this paper are on the basis of visible light. Sandwiched between the two electrodes are an array of cells that are filled with polyelectrolyte and a layer ofWO3 film of about 250 nm that consists of densely packed nanoparticles (Fig. 7d). The distance between the two electrodes is around 20 mm. As demonstrated in Fig. 7e, the fully packaged EC device still has a transmittance of more than 70%.

The NG has two different polymer layers between which a cavity is sustained by a spacer. Owing to the coupling of contact charging and electrostatic induction, electricity generation is achieved by a cyclic process of contact and separation between two polymer films. The performance of the NG is characterized by measuringopen-circuit voltage and short-circuits current.

An integrated module is presented in this work in the form of a combination of a nanoparticle-WO3 filmelectrochromic device and a nanogenerator, for demonstrating the potential of monochrome self-powered displays. This self-powered EC-device showed desirable ER times and high CE values. Furthermore, the EC device can be made on a flexible substrate and integrated with our flexible nanogenerator to be a kind of wearable device.

6. Transparent flexible nanogenerator as self-powered sensor for transportation monitoring

In this work, we fabricated transparent flexible nanogenerators (NGs) by employing flexible polydimethylsiloxane (PDMS) substrate for the growth of ZnO nanowires. The fully packaged NG showed good transparency with a transmittance of 50–60% in the visible range. The output voltage andcurrentwas 8V and 0.6 mA, respectively, is corresponding to an output power density of ~5.3 mW/cm3. The NG also showed excellent robustness and could stably scavenge energy from the motion of a vehicle. Based on this characteristic, we demonstrated its application as a self-powered sensor for monitoring vehicle speed and detecting vehicle weight.

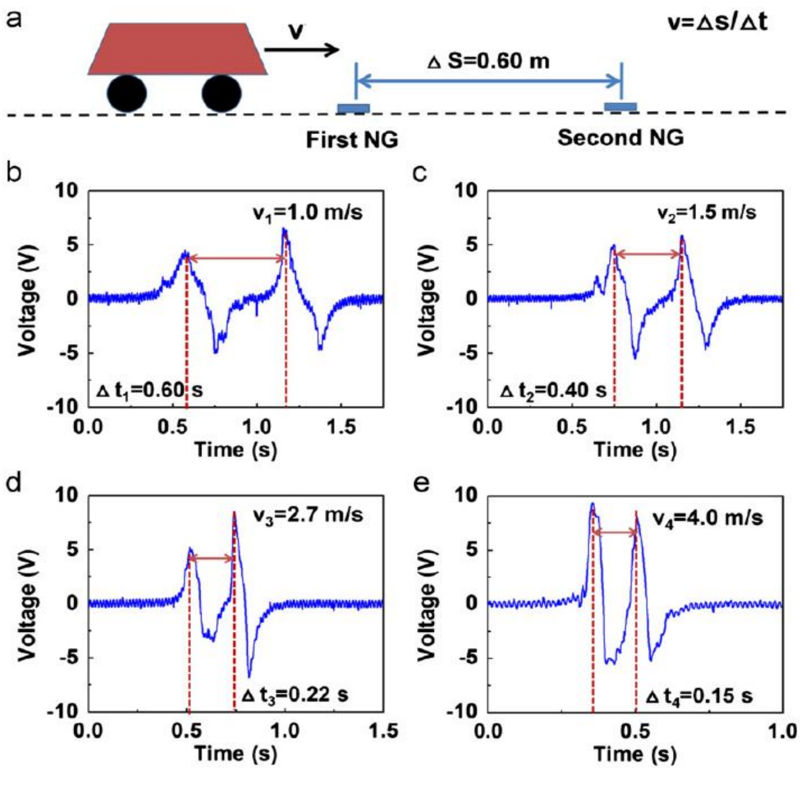

Figure 8 Application of the TFNG for self-powered transportation monitoring by detecting vehicle speed: (a) A schematic illustration showing the principle for measuring the vehicle speed on the road by the NG device. (b–e) The measured voltage–time relationship induced by vehicle tire with various speeds. The vehicle speed is calculated to be 1.0, 1.5, 2.7, and 4.0 m/s, respectively.

Figure 8a illustrates the basic principle of vehicle speed monitoring using NG. Generally, two NG devices with similar size were placed consequently along the rolling path of a moving vehicle. The distance between the two NG devices was fixed as Ds=0.6m. As the front tire of the vehicle rolled on the twoNGs subsequently, two successive voltage peaks could be recorded by the measurement system, with a measurable time interval of Dt. Assuming that the vehicle speed was Constant during this quick process, we were able to calculate The instant vehicle speed simply by v = Ds / Dt. Figure 8b–e Lists the measured voltage peaks under the rolling tire of the Vehicle at various speeds, from 1.0 m/s to 4.0 m/s. The high end detection limit was mainly determined by the sampling rate of the measurement system and the distance between the two NG devices (Ds). At current conditions (the sampling rate is $500s^{-1}$ and the NGs' distanceis 0.6m), the detection limit was ~300m/s and it was high enough for vehicle speed detection even in an expressway.

Theoretically, the output voltage of piezoelectric NG increases with the applied strain (or stress) on the structure. This is the principle for the vehicle weight monitoring using NG. Figure 9a shows the output voltage of NG driven by different vehicles with various curb weights, but at a constant and relatively low speed. It could be found that the output voltage increased with the vehicle weight. Figure 9b shows that the averaged output voltages had shown a linear relationship as a function of the curb weight of the vehicles. This result demonstrates the possibility of using NG as a self-powered sensor for monitoring the weight of vehicles on the road. Compared to traditional techniques for transportation monitoring, like speed camera and electronic balance, the NG-based speed and weight monitor has the following advantages: (1) it is a self-powered sensor and does not require external power source or specific maintenance and (2) it is transparent and flexible, which means it can be easily attached on to the road with any sort of environmental conditions, without interrupting the traffic.

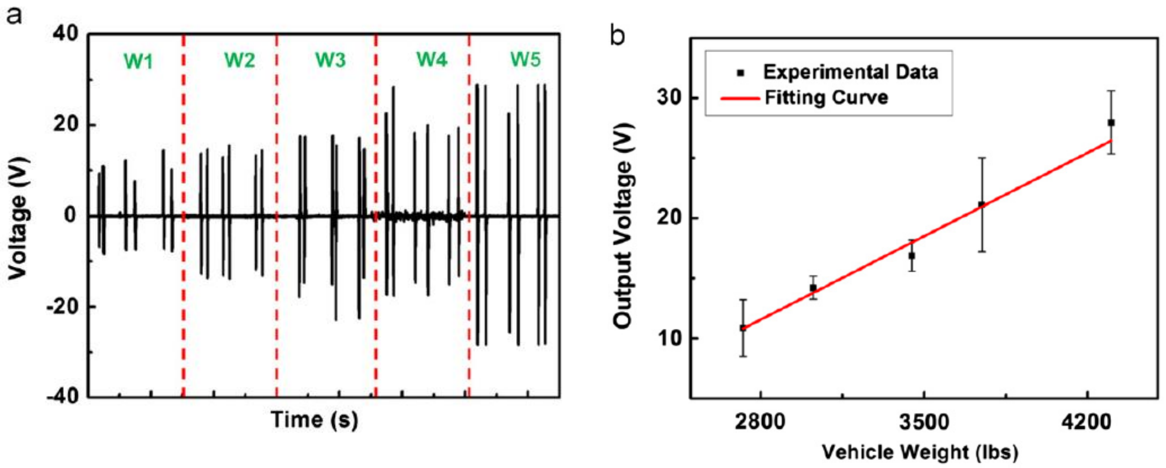

Figure 9 Application of the TFNG as self-powered pressure sensor for monitoring the vehicle weight: (a) Measured output voltages of NG device from tire rolling with various vehicle weights. It was observed that the output voltage increased with increasing vehicle weight. (b) Linear fitting of the average output voltage as a function of the vehicle weight.

7. Nanogenerators as an active sensor for vortex capture and ambient wind-velocity detection

In this work, we present a simple and practical composite structure for a nanogenerator (NG) or active-sensor for mechanical energy harvesting and vortex-based gas/liquid flow measurements. The composite design uses two kinds of piezoelectric material, ZnO and poly-(vinylidene fluoride) (PVDF). The power density and sensitivity of the composite NG are improved significantly. For energy recovery applications, the large electricity output of the NG results in a high working efficiency. Moreover, as an active nanosensor, the NG's high sensitivity and resolution makes it particularly suitable for detection of tiny deformations/mechanical-triggering. Utilizing the high performance NG, we demonstrate a simple and inexpensive method for flow measurement. As an active fluid sensor, the NG based vortex flow device (VFD) is developed for tiny ambient wind detection. Experimental results show that the NG-based VFD has a low working limit of only 0.6 m/s. While, commercial vortex flow meters for air generally work in the range from 6 m/s to 80 m/s. Moreover, the NG-based active VFD has the advantages of high noise tolerance, long life time, low system cost and no environment pollution risk. It should play important roles in environment air/water flow detection and oil/gas pipeline monitoring.

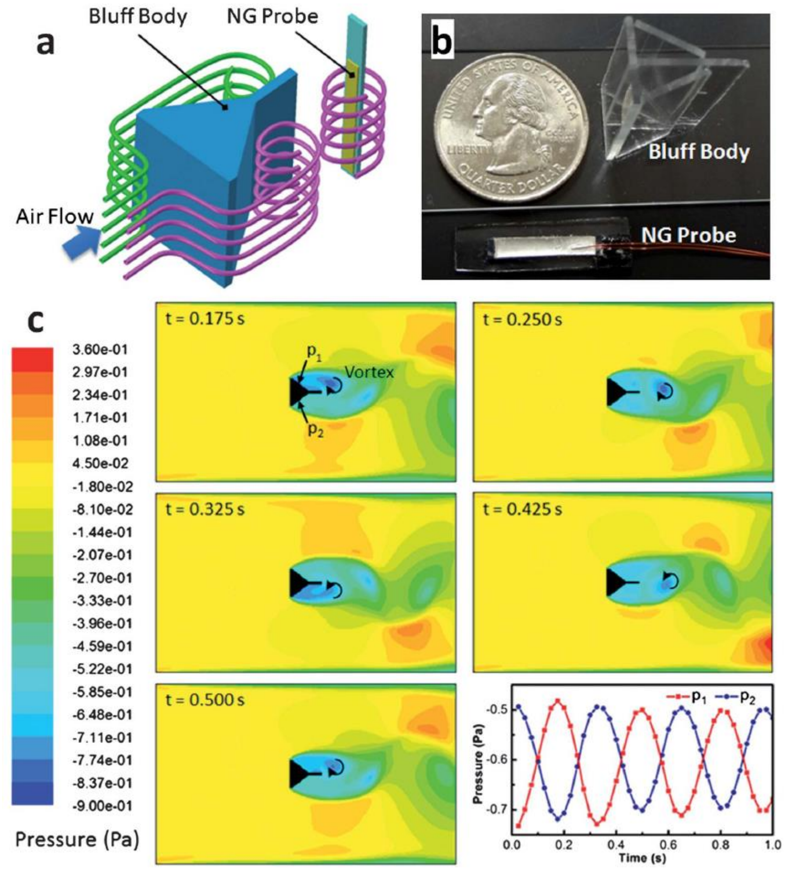

Figure 10 Schematic and simulation of the NG as an active sensor for detecting air flow. (a) Working principle of the vortex generation and capture. (b) Photo of the bluff body and the NG probe. (c) Transient pressure contours at different times, and curves of mean relative pressures on the two back faces.

With the NG as a vortex detector, an active VFD for super low airflow velocity measurement is demonstrated, which can be as low as 0.6 m/s. Fig. 10 a illustrates a schematic of the NG-based VFD. There are two main components in the system, the bluff body and the NG probe. The bluff body is designed as a triangle with a plate at its end. It is fixed in a steady and weak air flow, with its front face vertical to the flow direction. The active sensor is made of a NG bonded on a glass strip substrate. It is placed in the wake of the bluff body. According to the Karman vortex street principle, a row of vortices is generated on each side of the bluff body when the Reynolds number of the flow, Re, is in a certain range. The frequency of vortex shedding from the bluff body, f, depends on the input flow velocity, v, which is represented as

$$v = \frac{fd}{St}$$

where St is the Strouhal number, a non-dimensional number related to Re, d is the width of the bluff body. f is available by measuring the vortex induced local pressure variation with a NG probe. Thus, the flow velocity is obtained. A photo of the bluff body and NG probe is shown in Fig. 10 b. To understand the generation, distribution and strength of the vortices, computational fluidic dynamics is employed for vortex analysis. As shown in Fig. 2c, if we neglect the dimension and presence of the NG probe, a two-dimensional model of the bluff body is built for the simulation. The model of the bluff body is placed in the center of a rectangular calculation region, whose dimension is 134 mm X 80 mm. The left- and right-hand side edges of the rectangular region are set as the velocity inlet at 0.6m/s and the pressure outlet at atmosphere pressure, respectively. The unsteady flow induced by the bluff body is simulated with a time step of 25ms, and the pressure distributions in the calculation region at different times are shown in Fig. 10c. The low pressure in a localised area is caused by the rotation of the vortex, so that the position of the vortex is indicated. It is observed that a vortex with clockwise direction is generated at the upper face of the bluff body at t = 0.175 s and detaches from the bluff body gradually. The image at t = 0.25 s shows the completely detached vortex. Then, an anticlockwise vortex is formed at the lower face at t= 0.325 s, and subsequently it leaves the bluff body, as shown in the image at t = 0.425 s. The above process is repeated periodically after t = 0.5 s. The formation and detachment of vortices result in a pressure variation on the bluff body. The mean relative pressures on the upper and lower triangle edges, p1 and p2, are shown in the right bottom image in Fig. 2c, from which we can derive that the pressure variation is about 0.2 Pa and the frequency of vortex generation is around 3.25 Hz.

List of Publications and Significant Collaborations that resulted from your AOARD supported project:

a) papers published in peer-reviewed journals jointly between Korea and US researchers

1. Sangmin Lee[+], Sung-Hwan Bae[+], Long Lin[+], Seunghyun Ahn, Chan Park, Seung Nam Cha, Young Jun Park, Hyuk Chang, Sang-Woo Kim and Zhong Lin Wang* “Flexible hybrid cell for simultaneously harvesting thermal and mechanical energies”, Nano Energy

2. Sangmin Lee[+], Sung-Hwan Bae[+], Long Lin, Ya Yang, Chan Park, Sang-Woo Kim, Young Jun Park, Hyunjin Kim, Hyuk Chang and Zhong Lin Wang*” Super-flexible nanogenerator for energy harvesting from gentle wind and as active deformation sensor”, Adv. Func. Mater.

3. Keun Young Lee, Brijesh Kumar, Ju-Seok Seo, Kwon-Ho Kim, Jung Inn Sohn, Seung Nam Cha, Dukhyun Choi[*] Zhong Lin Wang[*] Sang-Woo Kim[*] “P-Type Polymer–Hybridized High-Performance Piezoelectric Nanogenerators”, Nano Letters, 12 (2012) 1959-1964.

4. Dukhyun Choi, Mi-Jin Jin, Keun Young Lee, Soo-Ghang Ihn, Sungyoung Yun, Xavier Bulliard, Woong Choi,[†] Sang Yoon Lee,[†] Sang-Woo Kim,[*,$] Jae-Young Choi,[*,†] Jong Min Kim,[†] and Zhong Lin Wang[*], “Flexible Hybrid Multi-Type Energy Scavenger”, Energy & Environmental Science, 4 (2011) 4607-4613.

b) papers published in peer-reviewed journals by US researchers

5. Xiaonan Wen, Wenzhuo Wu, Yong Ding, and Zhong Lin Wang, “Piezotronic Effect in Flexible Thin-film Based Devices" Advanced Materials, 2013, online DOI: 10.1002/adma.20130029.
6. Ya Yang, Hulin Zhang, Jun Chen, Sangmin Lee, Te-Chien Hou and Zhong Lin Wang, “Simultaneously harvesting mechanical and chemical energies by a hybrid cell for self-powered biosensors and personal electronics" Energy&Environmental Science, 2013, Online DOI: 10.1039/c3ee40764k.
7. Ya Yang, Hulin Zhang, Yan Liu, Zong-Hong Lin, Sangmin Lee, Ziyin Lin, Ching Ping Wong, and Zhong Lin Wang, “Silicon-Based Hybrid Energy Cell for Self-Powered Electrodegradation and Personal Electronics" ACS NANO, 2013, Online DOI: 10.1021/nn400361p
8. Long Lin, Qingshen Jing, Yan Zhang, Youfan Hu, Sihong Wang, Yoshio Bando, Ray P. S. Han and Zhong Lin Wang, “Elastic-spring-substrated nanogenerator as an active sensor for self-powered balance" Energy & Environmental Science, 2013, 6(4), 1164-1169
9. Zhong Lin Wang, Guang Zhu, Ya Yang, Sihong Wang, and Caofeng Pan, “Progress in nanogenerators for portable electronics" Materials Today, 2013, **15**, 12.
10. Ya Yang, Hulin Zhang, Sangmin Lee, Dongseob Kim, Woonbong Hwang, and Zhong Lin Wang, “Hybrid Energy Cell for Degradation of Methyl Orange by Self- Powered Electrocatalytic Oxidation" Nano Letters, 2013, 13 (2), pp 803–808.
11. Ya Yang, Zong-Hong Lin, Techien Hou, Fang Zhang and Zhong Lin Wang, “Nanowire-Composite based Flexible Thermoelectric Nanogenerators and Self-Powered Temperature Sensors" Nano Research, 2012, Volume 5, Issue 12, pp 888-895.
12. Ya Yang, Sihong Wang, Yan Zhang, and Zhong Lin Wang, “Pyroelectric Nanogenerators for Driving Wireless Sensors" Nano Letters, 2012, 12 (12), pp

6408–6413.

13. Zhong Lin Wang and Wenzhuo Wu, “Nanotechnology-Enabled Energy Harvesting for Self- Powered Micro-/Nanosystems" Angewandte Chemie, 2012, Volume 51, Issue 47, pages 11700–11721.
14. Xiaohong Yang, Guang Zhu, Sihong Wang, Rui Zhang, Long Lin, Wenzhou Wua and Zhong Lin Wang, “A self-powered electrochromic device driven by a nanogenerator" Energy & Environmental Science,2012, 5, 9462.
15. Ya Yang, Yusheng Zhou, Jyh Ming Wu, and Zhong Lin Wang, “Single Micro/Nanowire Pyroelectric Nanogenerators as Self-Powered Temperature Sensors", ACS NANO, 2012, 6 (9), pp 8456–8461.
16. Long Lin, Youfan Hu, Chen Xu, Yan Zhang, Rui Zhang, Xiaonan Wen, Zhong Lin Wang, “Transparent flexible nanogenerator as self-powered sensor for transportation monitoring" Nano Energy, 2012, 2(1), 75-81.
17. Rui Zhang, Long Lin, Qingshen Jing, Wenzhuo Wu, Yan Zhang, Zongxia Jiao, Liang Yan, Ray P. S. Hanc and Zhong Lin Wang, “Nanogenerators as an active sensor for vortex capture and ambient wind-velocity detection" Environmental & Energy Science, 2012, 5 (9), 8528 – 8533.
18. Qing Yang, Ying Liu, Zetang Li, Zongyin Yang, Xue Wang, and Zhong Lin Wang, “Self-Powered Ultrasensitive Nanowire Photodetector Driven by a Hybridized Microbial Fuel Cell" Angewandte Chemie, 2012, 51 (26), 6443-6446.
19. Zhong Lin Wang, “Self-Powered Nanosensors and Nanosystems” Advanced Materials, 2011, 24 (2), 279.
20. Minbaek Lee, Joonho Bae, Joohyung Lee, Churl-Seung Lee, Seunghun Hong and Zhong Lin Wang, "Self-powered environmental sensor system driven by nanogenerators" *Energy Environ. Sci.*, 4, 3359.
21. Zetang Li and Zhong Lin Wang, "Air/Liquid-Pressure and Heartbeat-Driven Flexible Fiber Nanogenerators as Micro/Nano-Power Source or Diagnostic Sensors " *Adv. Mater.*, 2010, 23 (1), 84-89.
22. Zhong Lin Wang, "Toward self-powered sensor networks" *Nano Today.*, (2010) 5, 512—514.

Attachments: Publications a) 1-22.

DD882: As a separate document, please complete and sign the inventions disclosure form.